Correlations Between Structures and Spectra of Protonated Water Clusters

Journal:	*The Journal of Physical Chemistry*
Manuscript ID	jp-2023-073387.R1
Manuscript Type:	Special Issue Article
Date Submitted by the Author:	19-Dec-2023
Complete List of Authors:	Finney, Jacob; University of Washington, McCoy, Anne; University of Washington, Department of Chemistry

Correlations Between Structures and Spectra of Protonated Water Clusters

Jacob M. Finney[a] and Anne B. McCoy *

Department of Chemistry, University of Washington, Seattle, WA 98195, USA

E-mail: abmccoy@uw.edu

Phone: 206-543-7464

[a]Current Affiliation: Department of Chemistry, Tacoma Community College, Tacoma, Washington 98466, USA

December 19, 2023

Abstract

Badger's rule-like correlations between OH stretching frequencies and intensities, and the OH bond length are used to develop a spectral mapping procedure for studies of pure and protonated water clusters. This approach utilizes the vibrationally averaged OH bond lengths, which were obtained from diffusion Monte Carlo (DMC) simulations that were performed using the general potential developed by Yu and Bowman. Good agreement is achieved between the spectra obtained using this approach and previously reported spectra for $H^+(H_2O)_n$ clusters, with $n = 3, 4$ and 5, as well as their perdueturated analogues. The analysis of spectra obtained by this spectral mapping approach support previous work that assigned the spectrum of $H^+(H_2O)_6$ to a mixture of Eigen and Zundel-like structures. Analysis of the calculated spectra also suggests a reassignment of the frequency of one of the transitions that involves the OH stretching vibration of the OH bonds in the hydronium core in the Eigen-like structure of $H^+(H_2O)_6$ from 1917 cm^{-1} to roughly 2100 cm^{-1}. For $D^+(D_2O)_6$, comparison of the measured spectrum to those obtained using the spectral mapping approach suggests that the carrier of the measured spectrum is one or more of the isomers of $D^+(D_2O)_6$ that contain a four-membered ring and two flanking water molecules. While there are several candidate structures, the two flanking water molecules most likely form a chain that is bound to the hydronium core.

Introduction

Assigning vibrational spectra of medium-sized clusters that are held together by hydrogen bonds has represented a long-standing challenge for theoretical and computational approaches.[1–6] Early studies focused on using scaled harmonic calculations to provide assignments.[7,8] The challenge in applying this approach to systems that include strong ionic hydrogen bonds comes from the large variability of the anharmonicities of the OH vibrations depending on the strength of the hydrogen-bonding interaction. For example, if we consider the ratio of the harmonic frequencies to the fundamental frequencies obtained from the assignment of the spectrum of $H^+(H_2O)_5$, we find that the ratios for the three vibrations that are assigned to the OH vibrations in the hydronium core range from 0.770 to 0.935.[2,9]

Second order vibrational perturbation theory (VPT2) has evolved into a method of choice for including anharmonicity in semi-rigid systems.[10–15] While this approach is effective in reproducing the anharmonic frequencies and intensities for vibrations that are well-described as perturbed harmonic oscillators, the approximation breaks down for hydrogen-bonded systems.[3,6] This is particularly notable for ionic hydrogen bonds between a hydronium ion and water molecules where the large anharmonicity of the OH stretching vibrations and strong couplings of these vibrations to low-frequency motions that affect the strength of the hydrogen bonds can result in energies of vibrationally excited states being calculated to be lower than the calculated zero-point energy.[3,16] This is also illustrated by $H^+(H_2O)_5$, where the reported differences between the VPT2 and measured values for the higher frequency OH stretching vibrations of the hydronium core near 2850 cm^{-1} are smaller than 20 cm^{-1}, while deviations larger than 250 cm^{-1} are found for the much more anharmonic lower frequency OH stretching vibration at 1890 cm^{-1}.[2]

These problems can be avoided by performing large-scale variational calculations, but the large density of vibrational states can make such calculations very challenging. Even in cases where such

calculations can be performed either using multi-configuration time-dependent Hartree (MCTDH) approaches or vibrational configuration-interaction calculations that are based on the states obtained from self-consistent field calculations (VSCF/VCI),[16–20] the assignment of the spectra remains a challenge. An attractive alternative is to use reduced dimensional approaches to explore spectra.[21,22] While studies of this type may be able to approximately capture the position of the band origins for the OH stretching vibrations, they will fail to fully capture the couplings between the OH stretching vibrations and the lower-frequency vibrations. Calculations of the vibrational dynamics of these protonated water clusters are also challenging for the nuclear-electronic orbital (NEO) approaches,[23] although recent work in the development of the CNEO approach by Yang and co-workers looks like a promising alternative.[24–27]

A complementary approach to those described above involves using the ground state probability amplitude to obtain insights into the spectrum of the protonated water clusters. In a series of studies, we developed such an approach in which we approximate the integrals that are needed to evaluate the excited state energies and matrix elements of the dipole moment operator using the ground state probability amplitude obtained from diffusion Monte Carlo (DMC) calculations.[28–30] We used this information to obtain transition frequencies and transition moments, which were then used to evaluate spectra. The resulting spectra for protonated water dimer, trimer and tetramer as well as $OH^-\cdot H_2O$ were shown to be in comparable agreement with experiment when compared to the results of VSCF/VCI and MCTDH calculations. While these results are encouraging, the approach requires careful construction of the internal coordinates, and this becomes more complicated as we consider larger clusters that contain ring structures.

A related, and somewhat simpler, approach involves mapping transition frequencies and intensities to structural features of the system of interest. For example, in a study of changes in the spectrum of the protonated water tetramer upon complexation with H_2, N_2, CO and one or two water molecules Wolke *et al.* showed that the frequencies of the hydrogen-bonded OH stretching vibrations could be correlated to the distance between the oxygen atoms in the donor and acceptor water molecules.[2] While such a correlation is not surprising, it provides an approach for mapping

the spectrum onto structural parameters. Likewise, through a series of studies, Xantheas and co-workers illustrated a linear relationship between the shift in the OH bond length and the shift in the frequency of the OH oscillator in a variety of hydrogen-bonding environments,[31,32] demonstrating a similar correlation to the one made by Badger that related shifts in diatomic bond lengths and the force constants.[33] The ratio of these shifts in the harmonic frequencies to the shift in the associated equilibrium OH bond lengths was shown to be approximately -19 cm^{-1} / 0.001 Å. Somewhat surprisingly, this ratio has been found to be independent of the level of electronic structure theory used for the calculations of the equilibrium geometries and harmonic frequencies. It is also insensitive to whether the harmonic frequencies, ω, are correlated to the equilibrium bond lengths, r_e, or the anharmonic frequencies, ν, are correlated to the zero-point averaged bond lengths, r_0.[34] In the latter case, both the anharmonic frequency and the zero-point averaged OH bond lengths were evaluated using VPT2. In a more recent study, Xantheas and co-workers identified a similar relationship for the hydronium ion.[35] Interestingly, the same proportionality constant of approximately -19 cm^{-1} / 0.001 Å applies to the OH bonds in both water and hydronium when they are compared to the appropriate reference. In analyzing these relationships for water clusters, we showed that we could relate the linear relationships between the OH bond lengths and frequencies to the response of these quantities to the local electric field,[34] thereby connecting the above treatment to the spectral mapping approaches that Skinner, Geissler and others have used to interpret the spectrum of water, both in bulk and for water clusters.[36–41]

The above relationship only provides information about the expected positions of peaks in the spectra. Modeling spectra also requires information about the intensities of these transitions. Work on hydrogen-bonded systems, particularly water clusters, has shown that there is also a linear relationship between the intensities and the frequencies of the OH stretching transitions.[42,43] Additionally Kananenka and Skinner showed that they could extend their spectral maps to include intensity information.[38] They used these maps to reproduce the spectrum of the book form of water hexamer that had been reported by Johnson and co-workers.[44] These results indicate that we should be able to obtain a good approximation with the anharmonic vibrational frequencies of OH

oscillators in either hydronium or water from the zero-point averaged OH bond lengths obtained using the accurate ground state probability amplitudes, for example those obtained from DMC calculations.

In the present study, we apply such a mapping approach to the assignment of the measured spectra for protonated water clusters. The developed maps are used to study the spectra of protonated water clusters with up to six water molecules. Of particular interest is the protonated water hexamer, where changes in the measured spectra upon deuteration indicate that different combinations of isomers are contributing to the reported spectra of $H^+(H_2O)_6{\cdot}H_2$ and $D^+(D_2O)_6{\cdot}D_2$. The approach is calibrated for smaller clusters, where the assignment of the spectrum is more straightforward, and the results are compared to those obtained using scaled harmonic and VPT2 approaches.

Methods

Diffusion Monte Carlo (DMC)

The approach described below requires accurate ground state probability amplitudes, which can be used to obtain vibrationally averaged values for structural parameters, for example OH bond lengths. These will be obtained using DMC. For the protonated water clusters with three or four water molecules, e.g. **3H**, **3D**, **4H-E**, and **4D-E**, we use the probability amplitudes obtained as part of a previous study,[45] while for clusters containing five and six water molecules, we follow the protocol used in our recent study of the **6H** clusters.[6]

In the above and the discussion that follows, we differentiate the protonated water clusters using ***n*H-isomer label** and ***n*D-isomer label** for a particular isomer of $H^+(H_2O)_n$ and $D^+(D_2O)_n$, respectively. In this notation, **E** is used to denote an Eigen-form of protonated water clusters, in which a hydronium ion is solvated by $n-1$ water molecules. We use **Z** to denote the H_2O-H^+-OH_2 Zundel-form of the ion, in which the excess proton is shared between two water molecules,[46,47] and the Zundel core is solvated by the $n-2$ remaining water molecules. Finally **T** is used to denote

a four-member ring structure. This notation differs from that was used in previous studies of **5H**,[9] and where there are differences we will note the naming scheme used in that study as well.

The details of DMC and our implementation of guided DMC for water clusters can be found elsewhere.[6,45,48–54] In this work, we use the potential energy surface that was developed by Yu and Bowman.[20] At the end of the simulation, we obtain a distribution of structures of the ion of interest, which provides a Monte Carlo sampling of the ground state wave function. We refer to the members of this distribution as *walkers*. The calculation of expectation values requires a way to evaluate the value of the wave function at each of the Monte Carlo sampling points. Suhm *et al.*[49] and Barnett *et al.*[50] have shown that this can be achieved using descendent weighting, in which the number of descendants of each walker is tabulated over a specified simulation time. The number of descendants for the kth walker is represented by w_k. Using these weights, the expectation values of atom-atom distances are obtained by evaluating

$$\langle r_{ij} \rangle = \sum_{k=1}^{N} r_{ij}(\mathbf{x}_k) w_k \tag{1}$$

where the summation is over the N individual walkers, and $\mathbf{x}_k$ provides the coordinates of the kth walker. Additional details about the implementation of DMC for the present study are provided in the Supporting Information.

Harmonic and VPT2 Calculations

In developing the mappings used in this study and generating spectra based on scaled harmonic and vibrational perturbation theory (VPT2) calculations, we optimized the structures and evaluated the harmonic frequencies and VPT2 frequencies and intensities at the MP2/aug-cc-pVTZ(-d) level of theory and basis. Due to the size of the calculations of the larger clusters, the $d-$orbitals were removed from the basis set for the hydrogen atoms. For the scaled harmonic calculations, scaling factors of 0.9531 and 0.9696 were used for the ions containing hydrogen and deuterium atoms, respectively. These values were chosen to match the positions of the calculated peaks associated

with the free OH stretching vibration in **6H-E2** and the free OD stretching vibration in **6D-T4** to the associated peaks in the reported spectra, which are at 3735 cm^{-1} and 2750 cm^{-1}, respectively.[2,55] A similar approach has been followed in previous studies of protonated water clusters.[56]

These harmonic calculations are also used in a harmonic localized normal mode treatment in which linear combinations of the normal modes that describe the OH stretching vibrations are taken in order to localize these motions to a single OH bond. This is achieved by following the approach described by Sibert and co-workers,[57,58] which is outlined in the Supporting Information. This treatment allows us to evaluate both the harmonic frequency associated with a single OH bond and the bilinear couplings that couple these motions. These couplings will become important in the description of the free OH region of the spectra. Because we have not included the transition moments for the free OH stretching vibrations in our model, we are not able to obtain relative intensities for these transitions. Instead, in plotting the spectra in this region we use a uniform intensity for all transitions involving unbound OH bonds.

To obtain the VPT2 spectra, calculations were performed in the subspace that included the OH stretching and HOH bending vibrations as the inclusion of the low-frequency vibrations can cause the expansions used in perturbation theory to diverge. The intensities are more sensitive to this behavior than the frequencies. As in perturbation theory, the corrections to the intensities of 1-0 transitions come in at second order, we have used the harmonic intensities in plots of the spectra. This approach is the same as what was used in a recent study of **6H**.[6] All of these calculations were performed using the Gaussian 16[59] program package.

Results and Discussion

Evaluation of Relationships Between OH Bond Lengths and Transition Frequencies and Intensities

We start by considering the correlations between the frequencies and intensities of OH stretching transitions and the calculated OH bond lengths. As noted above, previous work of Xantheas and

co-workers identified a linear relationship between the shifts in the calculated OH bond length and the vibrational frequency of the OH stretching vibration of an OH bond that is involved in a hydrogen bond compared to the corresponding values for an isolated water molecule.[31,32] This work also showed that the value of $d\omega_{\mathrm{OH}}^{(\mathrm{HOH})}/dr_{e,\mathrm{OH}}^{(\mathrm{HOH})}$ is independent of the level of electronic structure theory used to evaluate the equilibrium structure and the harmonic frequency. Recently they extended this exploration to hydronium, and showed that the value of $d\omega_{\mathrm{OH}}^{(\mathrm{H_3O^+})}/dr_{e,\mathrm{OH}}^{(\mathrm{H_3O^+})}$ is the same as that found for water.[35] That investigation explored a variety of levels of electronic structure theory and basis sets as well as the potential of Yu and Bowman used in the present study.[20] Finally, the work of Boyer, *et al.*[34] showed that for hydrogen bonded OH stretches in water clusters $d\nu_{\mathrm{OH}}^{(\mathrm{HOH})}/dr_{0,\mathrm{OH}}^{(\mathrm{HOH})} = d\omega_{\mathrm{OH}}^{(\mathrm{HOH})}/dr_{e,\mathrm{OH}}^{(\mathrm{HOH})}$, indicating that the anharmonic frequency and vibrationally averaged OH bond length follow the same trends as the harmonic frequency and the equilibrium OH bond length. Since the bond lengths and frequencies are referenced to those of either hydronium or water, we will use a superscript of either $(\mathrm{H_2O})$ or $(\mathrm{H_3O^+})$ to indicate which reference is being used.

Drawing from the above observations, we have calculated the shifts of the harmonic frequencies of the OH and OD oscillators and the corresponding equilibrium bond lengths for hydrogen-bound OH bonds in water and hydronium for a variety of water and protonated water clusters with up to six water molecules. The protonated water clusters include low-energy isomers that were identified in previous studies. The structures and names of these isomers are shown in Figure S1, while the subset of isomers that will be considered in the analysis of spectra are shown in Figure 1. Likewise, the structures of the neutral water clusters that were considered are shown in Figure S2. The calculated frequencies, which were evaluated at the MP2/aug-cc-pVTZ(-d) level of theory and basis, with the $d-$functions removed from the basis used to describe the hydrogen and deuterium atoms, are provided in the Supporting Information. These are the same structures that were used in the study of Boyer *et al*,[34] albeit with a slightly modified basis set. On the basis of the earlier studies, we expect that the value of $d\omega_{\mathrm{OH}}/dr_{e,\mathrm{OH}}$ obtained at the MP2/aug-cc-pVTZ(-d) level of theory can be used to obtain $\Delta\nu_{\mathrm{OH}}$ from $\Delta r_{0,\mathrm{OH}}$ values obtained from DMC calculations that were

performed using the potential of Yu and Bowman.[20]

One challenge in developing these spectral maps comes from the fact that the OH stretching vibrations are often collective in nature. In other words the normal modes involve displacements of several OH oscillators. On the other hand, the above correlations are based on Badger's rule and focus on isolated OH oscillators. As such, in developing the correlations between changes in bond lengths and frequencies, we calculate the OH stretch frequency for clusters in which we have replaced all but one of the hydrogen atoms with deuterium. Likewise to determine the frequency of the local OD stretching vibrations, the masses of all the hydrogen atoms except the one of interest are multiplied by four. This approximate doubling of the masses of the remaining hydrogen or deuterium atoms relative to the mass of the hydrogen or deuterium atom of interest provides an effective way to generate normal modes that are localized on a single OH or OD stretching oscillator. A similar approach was taken by Sibert and co-workers in their development of localized normal modes, and we use their approach to obtain quadratic coupling terms among the OH oscillators, as described in the Supporting Information.[22,57,58] The resulting local harmonic OH and OD stretching frequencies along with the corresponding OH bond lengths are provided in the EXCEL file that is provided as part of the Supporting Information.

Another challenge with the approach described above occurs when the OH bond length in hydronium becomes large, as large displacements of the OH bond length in the hydronium core correspond to situations where the ion is approaching a Zundel-like structure, in which the excess proton becomes equidistant from the donor and acceptor water molecules. In these cases, the potential experienced by the shared proton is very anharmonic and a model based on a perturbed hydronium ion breaks down. Of the ions considered in this study, the **6H-Z** ion is the only one that contains an OH bond length that exceeds 1.08 Å in its equilibrium geometry. In this case, $\Delta r_e \approx 0.2$ Å. As we do not expect the correlation we are developing to work well for this shared proton, in the application of the model we will limit ourselves to OH bonds that are displaced by no more than 0.1 Å from the length of the OH bond in the hydronium ion. Xantheas and co-workers considered a similar range of displacements of the OH bond lengths in their study of correlations

between the OH stretch frequency and OH bond length in clusters of a hydronium ion with up to five water molecules.[35]

Finally, while the analysis described above allows us to determine the frequencies and intensities of transitions involving OH bonds that are in hydrogen-bonding environments, it does not provide insights into the assignment of transitions involving the free OH oscillators. In most cases, these frequencies are close to the frequency of an OH bond in an isolated water molecule or hydronium ion. To model the spectrum in this region, we assume that the vibrational frequencies of the free OH oscillators are the average of the symmetric and antisymmetric stretches of the isolated water molecule or hydronium ion, and reintroduce the quadratic couplings between these oscillators that were obtained when we evaluated the localized normal modes. The values of the resulting bilinear couplings are shaded in blue in the Excel file that is included in the Supporting Information. For this spectral region, all transitions are given equal intensity, and the value of the intensity was chosen to allow comparison with the experimental spectrum. As such, the relative intensities of the transitions associated with the free OH oscillators are not expected to match the observed pattern in the measured spectra.

The results of this analysis are provided in Figure 2. Open orange circles are used to report results for water, while filled blue circles show the results for hydronium. In panels A and B, we report the change in the harmonic frequency of the isolated OH oscillators from their values in an isolated water molecule or hydronim ion, plotted against the shift in the corresponding value of the OH bond length in the optimized structure of the cluster. These data are fit to a line that goes through the origin, and the equation for the fit line is reported in the inset. The parameters are provided in Table 1, while the reference values for the OH bond lengths and harmonic frequencies are provided in Table 2. As expected from previous studies,[34,35] the slopes for both hydronium and water, plotted in Figure 2A, are close to -19 cm^{-1}/(0.001 Å).[31,32,34,35] Figure 2B provides the corresponding information for the OD stretching vibrations. As with the OH stretching vibrations, the slopes obtained for D_2O and D_3O^+ are nearly identical. Additionally, they are roughly $1/\sqrt{2}$ times the values obtained for the OH stretches. This is consistent with the decrease in the OD

harmonic frequency (compared to OH) by a factor of $\sqrt{2}$ while, based on the Born-Oppenheimer approximation, the equilibrium bond lengths are independent of mass. In a previous study, we found that anharmonic calculations of the OH stretching frequency and $r_{0,\mathrm{OH}}$ values in water yield similar slopes. We have repeated this analysis by comparing shifts of the values of $r_{0,\mathrm{OH}}$ and anharmonic frequencies for hydrogen-bonded OH stretching vibrations in the hydronium core. The results of this analysis are provided in Figure S3. these results show the same slope of -19.1 $\mathrm{cm}^{-1}/(0.001$ Å) as we obtained from the harmonic analysis. This slope differs from the slope obtained by relating experimental frequencies of the OH stretching vibrations of a solvated hydronium with the equilibrium OH bond length due to the non linearity of the anharmonic corrections to the frequencies, noted above.[60]

In the remaining two panels of Figure 2, we plot the calculated harmonic intensities, obtained from the calculations of the partially deuterated clusters as functions of the displacement of the OH bond lengths relative to an isolated water molecule or hydronium ion. In agreement with previous studies[42,43] the intensities of the OH stretching vibrations in water increase roughly linearly with the length of the donor OH bond. Since the intensities of the fundamental transitions involving the OH stretching vibration show a linear dependence on the hydrogen bond length, the results plotted in orange and blue in panels C and D of Figure 2 can be fit to a line, and the parameters are provided in the plot and in Table 1.

Comparison of Spectra

With the above correlations in hand, we can use the calculated vibrationally averaged OH bond lengths obtained from DMC simulations to determine the expected frequencies and intensities of the transitions in water and protonated water clusters that involve OH stretching vibrations. The calculated values of the vibrationally averaged OH bond lengths, $r_{0,\mathrm{OH}} \equiv \langle r_{\mathrm{OH}} \rangle_0$ are obtained from the DMC calculations and are provided in Tables S3-S6. The corresponding equilibrium bond lengths and harmonic frequencies can be found in Tables S24, S26, S32-S35 and S44-S49. In developing the correlations used in this study we only considered the OH bonds that were

displacements of up to 0.1 Å compared to the OH bond lengths in an isolated water molecule or hydronium ion. As such, we cannot use the frequency mapping approach to predict frequencies of the shared proton stretching vibrations when the displacement of the OH bond is larger than 0.1 Å, as is the case for the vibrationally averaged bond lengths of one of the OH bonds in **5H-E1**, **6H-T2**, and **6H-Z**.

While the calculated equilibrium bond lengths of the OH bonds for **5H-E1** and **6H-T2** were all within 0.1 Å of the equilibrium OH bond length in hydronium, when zero-point energy is introduced one of the OH bond lengths in the hydronium core of each of these ions became more than 0.1 Å larger than the zero-point averaged OH bond length in hydronium reported in Table 1. Likewise, the model developed in the present study treats all of the OH stretching vibrations as localized oscillators (as opposed to collective normal modes). With the exception of **3H** and **4H**, where two or three of the OH oscillators are equivalent by symmetry, each of the hydrogen-bound OH oscillators feels a unique OH bonding environment, and the OH oscillators are expected to remain localized. Likewise, because the model focuses on hydrogen-bonding environments, it cannot describe the free OH oscillators, and this region is modeled by introducing bilinear couplings between the OH oscillators, using the frequencies obtained for OH oscillators in an isolated water molecule or hydronium ion. Finally, the model cannot describe overtones or combination transitions involving lower-frequency vibrations. This final limitation also affects the scaled harmonic and the reported VPT2 spectra, which only consider the OH stretching and HOH bending vibrations. With these limitations in mind, the discussion that follows focuses on agreement between calculated and measured peaks. Structures that have predicted transitions in regions where there is no intensity in the measured spectrum will be considered unlikely candidates for being the carrier of the reported spectra.

The results of this analysis for $n\mathbf{H}$, $n = 3-5$, are plotted with the blue traces in Figure 3. These results are compared to the results of scaled harmonic calculations (green trace) and the results of VPT2 calculations that focus on the OH stretching and HOH bending vibrations, as described above (red trace). In many cases the anharmonic intensities deviate significantly from the

harmonic values for $\Delta v = 1$ transitions. We believe that this reflects, at least in part, challenges with small denominators in the second order correction to the wave functions that are used to calculate these intensities.[15,61] For this reason, the intensities plotted for the VPT2 spectra in Figure 3 are those obtained from the harmonic calculations. The bottom trace provides the previously reported measured spectrum.[4,9,62] The geometries of the isomers used in the construction of the calculated spectra are shown at the top of the panel.

The plot in panel A of Figure 3 shows the comparison of the measured and calculated spectra of **3H**. The assignment of this spectrum is complicated by the near degeneracy between the hydrogen-bound OH stretches in the hydronium core and states with two quanta of excitation in vibrational motions that break the hydrogen bonds. The arrows in the spectra for **3H** and **3D** provide the previously reported locations of the centroid of the OH or OD 1-0 bands at 2100 and 1664 cm^{-1}, respectively.[4] The analysis that is based on the relationships between OH bond lengths and the frequencies and intensities provided in Figure 2 (blue) produces a peak, identified as 1-2, that is about 100 cm^{-1} larger than the transition indicated by the arrow in the experimental spectrum. Compared to the scaled harmonic calculation (green) the spectral mapping method prediction is significantly closer to peak in the the experimental spectrum that has been assigned to this transition. The calculated transition from VPT2 overestimates the anharmonicity and predicts a peak that is about 100 cm^{-1} lower than the transition in the experimental spectrum. Upon deuteration (panel E) the agreement between the results of the spectral mapping method (blue) and experiment has improved. Specifically, the peak identified as 1-2 in the blue spectrum is nearly on top of the arrow that shows the position of the centroid of intensity in the experimental spectrum.[4]

Panel B in Figure 3 shows the calculated and experimental spectra of **4H-E**. The spectral mapping method (blue) predicts that the shared proton transition, peak labeled 1-3, is at 2848 cm^{-1}, which agrees well with the scaled harmonic calculation (green) but is still about 100 cm^{-1} higher than the transition in the experimental spectrum. The VPT2 calculation overestimates the anharmonicity of this transition, resulting in a calculated peak that is lower in frequency than the most intense feature in the experimental spectrum. Comparing the calculated and measured spectra for

4D-E, we find the same trends as we observed for **4H-E**, albeit with smaller shifts between the various calculations.

Panels C and D in Figure 3 compare the calculated spectra of two low energy isomers of **5H** to the experimental spectrum. As part of the study where the experimental spectrum of this species was reported, Fagiani *et al.* also reported that the **5H-E1** (referred to as the branched isomers in their study) and the **5H-T** isomer (referred to as the ring isomer in their study) differed in energy by less than 1 kJ/mol once zero-point energy was accounted for at the harmonic level.[9] Their calculations were performed at the B3LYP-D3/aug-cc-pVTZ level of theory and basis set, and the relative energies were corrected based on single point calculations, which were performed at the CCSD(T)/aug-cc-pVTZ level of theory/basis set. Similar values for the relative energies are obtained from the MP2/aug-cc-pVTZ(-d) calculations performed in the present study (see Table S1). That the **5H-E1** isomer is lower in energy than the **5H-T** isomer is consistent with the observation that the agreement between the calculated and measured spectra for **5H-E1** (panels C and G) is significantly better than the agreement found for the **5H-T** isomer (panels D and H).

Focusing on the spectra for **5H-E1** (panel C) the large peak in the spectrum obtained using the spectral mapping method is at 3107 cm^{-1} (peak 2-3). It is about 140 cm^{-1} higher than the experimental peak. It is also higher than both the scaled harmonic (green) and VPT2 (red) calculations predict. Close examination of the spectral mapped spectrum shows that there is no peak associated with the OH bond labeled as 1. This is because the vibrationally averaged length of this OH bond, $r_{0,OH}$, is more than 0.1 Å larger than the corresponding bond length in hydronium, putting it outside the range of applicability of the model. This transition has been previously assigned to the peak at 1890 cm^{-1} in the black trace. Upon deuteration, the spectrum for the E1 isomer is seen to be in better agreement with the measured spectrum compared to its all hydrogen counterpart.

Overall, we find that the spectral mapping approach provides good agreement with the measured spectra for these protonated water clusters, providing us with the confidence to extend the approach to larger clusters.

Free OH Stretch Region

As noted above, the spectral mapping approach cannot be used to model the spectrum in the free OH stretching region. On the other hand, we do not expect that the frequencies of the OH stretching vibrations will be significantly altered from the values for local OH oscillators in water or hydronium. On the basis of these observations, we model this spectral region using an approximation in which the anharmonic OH stretching frequencies are obtained from calculations using accurate potential surfaces,[63,64] and are reported in Table 1. Some of the flanking water molecules will have two free OH bonds, and in these cases, we introduce a bilinear coupling between these two OH vibrations. This results in a model Hamiltonian,

$$H = \nu_{\mathrm{OH}} (n_1 + n_2 + 1) + \lambda \left(a_1^{\dagger} a_2 + a_1 a_2^{\dagger} \right) \tag{2}$$

which resembles the harmonically coupled anharmonic oscillator model described by Halonen and Child.[65,66] In this model, ν_{OH} provides the anharmonic frequency of the OH oscillator, while λ provides the quadratic coupling between the two OH oscillators. The value of λ is obtained by localizing the normal modes associated with the OH stretching vibrations, following the approach described by Sibert and co-workers[22,57,58] and summarized in the Supporting Information.

The resulting spectra are shown with purple dashed lines in the DMC panels of Figure 3. The transitions are labeled as (*a*)ntisymmetric and (*s*)ymmetric. The free OH in a (*h*)ydronium core is labeled as *h*, while a single free OH in water is labeled (*l*)ocal. The relative intensities of the resulting symmetric and antisymmetric stretches will depend on the vector sums (or differences) between the transition moments of the two OH oscillators. As we do not have a direct way to obtain these transition moments, we have elected to simply scale a constant intensity by the number of OH vibrations at a particular frequency. With that in mind, the relative positions of the peaks in the OH stretching region seen for the calculations based on the spectral mapping approach agree well with those in the experimental spectrum. The exception is for **5H-T**, which is not found to be the carrier of the observed spectrum.[9]

We have also used this approach to introduce couplings between the hydrogen-bonded OH stretching vibrations. The results of this analysis are shown as purple dashed lines of Figure S4. The introduction of these couplings has the largest effect on the calculated spectrum of **3H**, where the two peaks that are associated with the hydrogen-bound OH stretching vibrations in the hydronium core are split by 145 cm^{-1}. Once split, the lower frequency peak shows better agreement with the arrow in the experimental spectrum. On the basis of harmonic calculations of the spectrum of this ion, we expect that the lower-frequency peak will carry more intensity than the higher frequency one.

Spectra for 6H and 6D

With the insights from the smaller protonated water clusters, we consider the spectra of **6H** and **6D**. In the case of **6H,** previously reported double resonance experiments have allowed workers to deconvolute the observed spectrum into two contributions. The one shown in panel A of Figure 4 was assigned as corresponding to the **6H-E2** structure shown at the top of this column, while the spectrum shown in panel B was assigned to the **6H-Z** structure shown above this column. The spectrum for **6D** likely also has multiple contributions. The lack of a peak near 800 cm^{-1}, where we would expect to see a peak assigned to the displacement of the share proton in the **6D-Z** isomer, indicates that this isomer is unlikely to contribute to the observed spectrum.

We start with the free OH region. For **6H-E2**, this region of the spectrum contains three peaks, consistent with a symmetric stretch, an antisymmetric stretch as well as a local OH stretch. This is also consistent with the structure and the corresponding spectrum obtained using the spectral mapping approach. In contrast the **6H-Z** spectrum contains only two peaks in the free OH region. This is consistent with the absence of a local OH stretching vibration in this structure. Examination of the spectrum for **6D** in the free OH region, we see one broadened and one narrow peak. This would be consistent with local OH stretching vibrations as well as symmetric and antisymmetric stretches. The broadening of the lower frequency component suggests that there might be multiple local OH stretching vibrations in water molecules that experience slightly different hydrogen-bonding en-

vironments. Such a situation would be more consistent with the **6D-T4** structure, which contains two types of symmetry distinct local free OH groups, than **6D-T2**, which contains only one local free OH vibration.

Shifting to the lower frequency region, which involves hydrogen-bonded OH stretching vibrations, we compare the predictions of the spectral mapping approach to the observed spectra. Starting with **6H-E2**, shown in the upper left, there are expected to be three types of hydrogen-bonding environments, those experienced by the OH bonds labeled 1 and 2, the OH bond labeled 3 and the two OH bonds labeled 4 and 6. The highest frequency transition among these will be that associated with OH bonds 4 and 6. The spectral mapping approach places these transitions at 3280 and 3299 cm^{-1}, which are in good agreement with the peak in the measured spectrum at 3312 cm^{-1} that has been assigned to this transition. Likewise, the transition involving the OH bond labeled 3 is calculated to be at 3147 cm^{-1}, which is in reasonable agreement with the transition at 3007 cm^{-1} that is assigned to this transition.[55] At the level of electronic structure theory used in this study, the VPT2 calculation underestimates the position of these transitions, placing them at 3242, 3223 and 2933 cm^{-1}, respectively while the scaled harmonic calculations provide frequencies of 3316, 3310, and 3057 cm^{-1}, respectively.

The agreement between experiment and calculation for the remaining OH stretching transitions appears to be less good. Previous experimental[55] and computational[67] studies assign the transitions involving the OH bonds labeled 1 and 2 to peaks in the measured spectrum at 2425 and 1951 cm^{-1}, while VSCF/VCI calculations place these transitions at 2345 and 1991 cm^{-1}. The spectral mapping calculations predict transitions at 2351 and 2271 cm^{-1}, while VPT2 calculations give transitions at 2276 and 2064 cm^{-1} (with very large anharmonicities). If we introduce quadratic couplings among all of the OH stretching vibrations, these frequencies are reduced to 2344 and 2199 cm^{-1}, as shown in the spectrum plotted in blue in panel A of Figure S5. At first it seemed surprising that both frequencies decrease with the introduction of couplings. The lowering of these two frequencies is compensated for by an increase in the OH stretching frequencies of OH bonds in the flanking water molecules, particularly the OH bonds that form hydrogen bonds to a second

water molecule.

While the agreement between experiment and calculation for the higher frequency transition is very good, the discrepancy for the lower frequency transition is concerning and a comparison of the frequency of the lowest-frequency transition in **6H-E2** to the corresponding transition in **5H-E1** led us to question the assignment of the reported spectrum. Specifically **5H-E1** and **6H-E2** both contain at least one OH bond in the hydronium core that is solvated by a chain of two water molecules. In **5H-E1** this is the OH bond identified with the orange 1 above panel C of Figure 3, while for **6H-E2** they are the OH bonds identified with the orange 1 and 2 above panel A of Figure 4. From studies of other hydrogen-bonded systems,[2,68] we expect that the strength of the ionic hydrogen bond, and from that the red shift of the OH stretching frequency, will be higher when the OH bond is solvated by a chain of two water molecules compared to the situation when it is solvated by a single water molecule (as is the case for OH bonds 2 and 3 in **5H-E1** and OH bond 3 in **6H-E2**). This can be seen by comparing the frequency of the OH stretching vibration involving OH bond 1 in the inset of Figure 3 in **5H-E1** at 1899 cm^{-1} to the frequencies of the transitions assigned to excitation of the OH bonds labeled 2 and 3 at 2837 and 2883 cm^{-1}.[2] When two or more OH bonds are in stronger solvation environments, we expect that the vibrational frequency will be larger than the case when only one OH bond is in that environment. This can be seen by comparing the frequencies of, for example, the OH stretching vibrations of the hydronium core in **3H** and **4H-E**. On the basis of the above analysis, we expect that the transitions associated with OH bonds 1 and 2 in **6H-E2** would both be well-above the 1900 cm^{-1} frequency of the corresponding transition in **H5-E**. We also find that all of the calculations over-estimate the frequency of the transitions associated with OH bonds 1 and 2 in **6H-E2**. In contrast, most of the other features in the measured spectra lie between peaks in the corresponding VPT2 spectrum (red) and the spectrum that is obtained by applying the spectral mapping approach (blue). These observations led us to consider that the frequency of this transition should be closer to the value of 2271 cm^{-1} obtained by the spectral mapping approach. The above analysis would place the lowest-frequency transition in **6H-E2** associated with the OH stretching vibration in the hydronium core in a region of lower

signal to noise in the experimental spectrum. With this adjustment to the assignment, the feature near 2000 cm^{-1} would be assigned to transitions involving overtones and combinations of the HOH bends along with low-frequency vibrations that break the strong ionic hydrogen bonds between the hydronium core and the flanking water molecules. These transitions have been previously invoked to explain the structured band contour in the OH stretching region of **3H**.[4]

The above reconsideration of the assignment is consistent with several other calculations. For example, the spectra obtained from AIMD calculations reported by Heine *et al.*[55] shows no intensity between 1800 and 2000 cm^{-1}, but contains a broad peak spanning from 2150 to 2600 cm^{-1}. Classical calculations of spectra often do not capture transitions involving two or more quanta of excitation, supporting the possibility that the peak near 2000 cm^{-1} in the spectrum reflects higher-order transitions. We also performed several reduced-dimensional calculations of the OH frequencies of OH stretching vibrations of the hydronium core **5H-E1** and **6H-E2**. Details of these calculations can be found in the Supporting Information. While we do not expect these calculations to provide accurate frequencies, we are interested in the trends in the frequencies of the transitions involving OH oscillators that are solvated by one or two water molecules. As shown in the results provided in Table S2, the energy difference between the lower energy state of **6H-E2** that is solvated by a chain of two water molecules and the excited state of the OH stretch in **5H-E1** that is in a similar solvation environment is much larger than the 50 cm^{-1} that is expected based on the assignment of the experimental spectra for these ions

For the other isomers of **6H**, the agreement between the spectral mapping model and the spectrum of **6H-Z** is good, while the agreement for the other isomers is not as good. This is expected based on previous assignment of the spectrum.[6,55]

Shifting the discussion to the spectra of the various isomers of **6D**, we have already argued that the **6D-Z** isomer is not contributing to the observed signal. Likewise, consistent with previous studies, the calculated peaks associated with OD bonds 1 and 2 in the **6D-E2** isomer occur in a frequency range in which there is no intensity in the experimental spectrum. Consistent with our recent study that focused on VPT2 calculations,[6] improved agreement between the calculated and

measured spectra are obtained for both the **6D-T2** and **6D-T4** isomers. As with the other spectra considered in this study, the frequencies predicted from the spectral mapping analysis are typically larger than those anticipated by VPT2 calculations and lower than those anticipated by the scaled harmonic calculations. While the calculated spectrum for the **6D-T4** isomer does not recover the intensity between 1400 and 1600 cm^{-1}, this peak in the measured spectrum likely has contributions from two or more quanta transitions involving the DOD bend with low-frequency vibrations that break the strong ionic hydrogen bonds.

In plotting the spectra in Figures 3 and 4, we have chosen the axes for plotting the spectra of the deuterated ions so the frequency axes are scaled by roughly a factor of $\sqrt{2}$ relative to the fully hydrogenated species. This allows us to explore changes in the spectral envelope with deuteration. For the smaller systems, there is a clear correlation between peaks in the spectra of the hydrogen-containing ion and that for the fully deuterated ion. This is not the case when we compare the experimental spectra for **6H** and **6D**, black traces in panes C and G of Figure 4. Two notable differences are the peaks at 2050 cm^{-1} and another at 2588 cm^{-1} in the spectrum of **6D** that do not have corresponding features in the **6H** spectrum, and we focus on these features as we further consider the assignment of the spectrum of **6D**. Comparing the calculated and experimental spectra, we find that the calculated spectra for **6D-T2** in panel G and **6D-T4** in panel H show the best agreement when we focus on these two features. This is consistent with our previous study in which we noted that the VPT2 spectrum of **6D-T2** showed better agreement with the measured spectrum when compared to the VPT2 spectra obtained for **6D-E2** and **6D-Z**.[6] On the basis of these observations it appears that the carrier of the **D6** spectrum is likely an isomer that contains a four-membered ring, and the so-called T4 isomer appears to show slightly better agreement with the measured spectrum compared to the T2 isomer of **D6**.

Conclusions

In this study, we explored a spectral mapping approach that is based on the Badger's rule relationship between OH bond lengths and the vibrational frequencies associated with that OH bond. Previous studies demonstrated that changes in the vibrationally averaged value of the OH bond length could be mapped onto shifts in the frequency through a scaling factor of approximately -19 cm^{-1}/(0.001 Å).[34,35] We have demonstrated that this relationship holds for OH bonds in hydronium as well as water. We also extended the correlation to deuterated clusters as well as to the evaluation of intensities.

Once developed, the spectral mapping model was applied to a series of protonated water clusters, $H^+(H_2O)_n$ and $D^+(D_2O)_n$ with $n = 3-6$. The smaller clusters were used to validate the approach as their spectra had been assigned in previous studies.[2,4,62] For **6H** and **6D**, the approach was used in the assignment of these spectra[55] to isomers. In the case of **6H**, we revisited one of the assignments of the bands associated with OH stretching vibrations of the hydronium core of the Eigen-like isomer (**6H-E2**). We believe that the approach described in this contribution provides a powerful alternative to more demanding calculations as we consider at least the initial assignment of the spectra of water clusters.

Supporting Information

Additional details on numerical methods used including Diffusion Monte Carlo, VPT2, harmonic local mode and reduced dimensional calculation; Structures of the clusters considered in this study; Plot of the correlation of the anharmonic frequencies and $\langle r_{\mathrm{OH/D}} \rangle$ for H_3O^+; Additional calculated spectra that include bilinear couplings among all the OH vibrations; Relative energies of the **5H** isomers; Energies obtained from reduced dimensional calculation; Frequencies, intensities, and $\langle r_{\mathrm{OH/D}} \rangle$ used as inputs for the spectral mapping method; Harmonic and VPT2 frequencies and intensities for the isomers considered in this study; Equilibrium geometries and harmonic frequencies for the isomers considered in this study, evaluated using the potential of Yu and Bowman; Excel file containing OH/D bond lengths, harmonic and anharmonic frequencies, and intensities used in this study, the parameters used for the spectral maps, as well as the bilinear couplings obtained from local mode harmonic calculations.

Acknowledgements

The authors gratefully acknowledge the Department of Energy through the condensed phase and interfacial molecular science (CPIMS) program (DE-SC0021081) for support of this study of protonated water clusters and the chemistry division of the NSF (CHE-2154126) for the associated DMC methods development. Parts of this work were performed using the Ilahie cluster at the University of Washington, which was purchased using funds from a MRI grant from the National Science Foundation (CHE-1624430). This material is based in part upon work supported by the state of Washington through the University of Washington Clean Energy Institute.

References

(1) Headrick, J. M.; Diken, E. G.; Walters, R. S.; Hammer, N. I.; Christie, R. A.; Cui, J.; Myshakin, E. M.; Duncan, M. A.; Johnson, M. A.; Jordan, K. D. Spectral Signatures of Hydrated Proton Vibrations in Water Clusters. *Science* **2005**, *308*, 1765–1769.

(2) Wolke, C. T.; Fournier, J. A.; Dzugan, L. C.; Fagiani, M. R.; Odbadrakh, T. T.; Knorke, H.; Jordan, K. D.; McCoy, A. B.; Asmis, K. R.; Johnson, M. A. Spectroscopic Snapshots of the Proton-Transfer Mechanism in Water. *Science* **2016**, *354*, 1131–1135.

(3) Samala, N. R.; Agmon, N. The protonated water trimer and its giant Fermi resonances. *Chem. Phys.* **2018**, *514*, 164–175.

(4) Duong, C. H.; Yang, N.; Johnson, M. A.; DiRisio, R. J.; McCoy, A. B.; Yu, Q.; Bowman, J. M. Disentangling the Complex Vibrational Mechanics of the Protonated Water Trimer by Rational Control of Its Hydrogen Bonds. *J. Phys. Chem. A* **2019**, *123*, 7965–7972.

(5) Fournier, J. A.; Johnson, C. J.; Wolke, C. T.; Weddle, G. H.; Wolk, A. B.; Johnson, M. A. Vibrational spectral signature of the proton defect in the three-dimensional $H^+(H_2O)_{21}$ cluster. *Science* **2014**, *344*, 1009–1012.

(6) Finney, J. M.; Choi, T. H.; Huchmala, R. M.; Heindel, J. P.; Xantheas, S. S.; Jordan, K. D.; McCoy, A. B. Isotope Effects in the Zundel–Eigen Isomerization of $H^+(H_2O)_6$. *J. Phys. Chem. Lett.* **2023**, *14*, 4666–4672.

(7) Scott, A. P.; Radom, L. Harmonic Vibrational Frequencies: An Evaluation of Hartree-Fock, Møller-Plesset, Quadratic Configuration Interaction, Density Functional Theory, and Semiempirical Scale Factors. *J. Chem. Phys.* **1996**, *100*, 16502–16513.

(8) Alecu, I. M.; Zheng, J.; Zhao, Y.; Truhlar, D. G. Computational Thermochemistry: Scale Factor Databases and Scale Factors for Vibrational Frequencies Obtained from Electronic Model Chemistries. *J. Chem. Theory. Comput.* **2010**, *6*, 2872–2887.

(9) Fagiani, M. R.; Knorke, H.; Esser, T. K.; Heine, N.; Wolke, C. T.; Gewinner, S.; Schöllkopf, W.; Gaigeot, M.-P.; Spezia, R.; Johnson, M. A. et al. Gas Phase Vibrational Spectroscopy of the Protonated Water Pentamer: the Role of Isomers and Nuclear Quantum Effects. *Phys. Chem. Chem. Phys.* **2016**, *18*, 26743–26754.

(10) Sibert, E. L. Theoretical Studies of Vibrationally Excited Polyatomic Molecules Using Canonical Van Vleck Perturbation Theory. *J. Chem. Phys.* **1988**, *88*, 4378–4390.

(11) Barone, V. Anharmonic Vibrational Properties by a Fully Automated Second-Order Perturbative Approach. *J. Chem. Phys.* **2005**, *122*, 014108.

(12) Piccardo, M.; Bloino, J.; Barone, V. Generalized Vibrational Perturbation Theory for Rotovibrational Energies of Linear, Symmetric and Asymmetric Tops: Theory, Approximations, and Automated Approaches to Deal With Medium-to-Large Molecular Systems. *Int. J. of Quant. Chem.* **2015**, *115*, 948–982.

(13) Yang, Q.; Mendolicchio, M.; Barone, V.; Bloino, J. Accuracy and Reliability in the Simulation of Vibrational Spectra: A Comprehensive Benchmark of Energies and Intensities Issuing From Generalized Vibrational Perturbation Theory to Second Order (GVPT2). *Front. Astron. Space Sci.* **2021**, *8*, 665232.

(14) Franke, P. R.; Stanton, J. F.; Douberly, G. E. How to VPT2: Accurate and Intuitive Simulations of CH Stretching Infrared Spectra Using VPT2+K with Large Effective Hamiltonian Resonance Treatments. *J. Phys. Chem. A* **2021**, *125*, 1301–1324.

(15) Boyer, M. A.; McCoy, A. B. A flexible approach to vibrational perturbation theory Using Sparse Matrix Methods. *J. Chem. Phys.* **2022**, *156*, 054107.

(16) Hammer, N. I.; Diken, E. G.; Roscioli, J. R.; Johnson, M. A.; Myshakin, E. M.; Jordan, K. D.; McCoy, A. B.; Huang, X.; Bowman, J. M.; Carter, S. The Vibrational Predissociation Spectra of the $H_5O_2^+ \cdot RG_n$(RG=Ar,Ne) Clusters: Correlation of the Solvent Perturbations in the Free OH and Shared Proton Transitions of the Zundel Ion. *J. Chem. Phys.* **2005**, *122*, 244301.

(17) Vendrell, O.; Gatti, F.; Lauvergnat, D.; Meyer, H.-D. Full-dimensional (15-dimensional) quantum-dynamical simulation of the protonated water dimer. I. Hamiltonian setup and analysis of the ground vibrational state. *J. Chem. Phys.* **2007**, *127*, 184302.

(18) Vendrell, O.; Gatti, F.; Meyer, H.-D. Strong Isotope Effects in the Infrared Spectrum of the Zundel Cation. *Agew. Chem. Int. Ed.* **2009**, *48*, 352–355.

(19) Schröder, M.; Gatti, F.; Lauvergnat, D.; Meyer, H.-D.; Vendrell, O. The coupling of the hydrated proton to its first solvation shell. *Nature Communications* **2022**, *13*, 6170.

(20) Yu, Q.; Bowman, J. M. Communication: VSCF/VCI Vibrational Spectroscopy of $H_7O_3^+$ and $H_9O_4^+$ Using High-Level, Many-Body Potential Energy Surface and Dipole Moment Surfaces. *J. Chem. Phys.* **2017**, *146*, 121102.

(21) Yang, N.; Duong, C. H.; Kelleher, P. J.; McCoy, A. B.; Johnson, M. A. Deconstructing Water's Diffuse OH Stretching Vibrational Spectrum With Cold Clusters. *Science* **2019**, *364*, 275–278.

(22) McCoy, A. B.; Dzugan, L. C.; DiRisio, R. J.; Madison, L. R. Spectral Signatures of Proton Delocalization in $H^+(H_2O)_{n=1-4}$ Ions. *Faraday Discuss.* **2018**, *212*, 443–466.

(23) Fetherolf, J. H.; Pavošević, F.; Tao, Z.; Hammes-Schiffer, S. Multicomponent Orbital-Optimized Perturbation Theory with Density Fitting: Anharmonic Zero-Point Energies in Protonated Water Clusters. *J. Phys. Chem. Lett.* **2022**, *13*, 5563–5570.

(24) Xu, X.; Yang, Y. Constrained Nuclear-Electronic Orbital Density Functional Theory: Energy Surfaces with Nuclear Quantum Effects. *J. Chem. Phys.* **2020**, *152*, 084107.

(25) Xu, X.; Yang, Y. Full-Quantum Descriptions of Molecular Systems from Constrained Nuclear–Electronic Orbital Density Functional Theory. *J. Chem. Phys.* **2020**, *153*, 074106.

(26) Zhang, Y.; Xu, X.; Yang, N.; Chen, Z.; Yang, Y. Describing Proton Transfer Modes in Shared

Proton Systems with Constrained Nuclear–Electronic Orbital Methods. *J. Chem. Phys.* **2023**, *158*, 231101.

(27) Zhang, Y.; Wang, Y.; Xu, X.; Chen, Z.; Yang, Y. Vibrational Spectra of Highly Anharmonic Water Clusters: Molecular Dynamics and Harmonic Analysis Revisited with Constrained Nuclear-Electronic Orbital Methods. *J. Chem. Theory Comput.* Published ASAP, December 14, 2023.

(28) McCoy, A. B.; Diken, E. G.; Johnson, M. A. Generating Spectra from Ground-State Wave Functions: Unraveling Anharmonic Effects in the $OH^- \cdot H_2O$ Vibrational Predissociation Spectrum. *J. Phys. Chem. A* **2009**, *113*, 7346–7352.

(29) Guasco, T. L.; Johnson, M. A.; McCoy, A. B. Unraveling Anharmonic Effects in the Vibrational Predissociation Spectra of $H_5O_2^+$ and Its Deuterated Analogues. *J. Phys. Chem. A* **2011**, *115*, 5847–5858.

(30) DiRisio, R. J.; Finney, J. M.; Dzugan, L. C.; Madison, L. R.; McCoy, A. B. Using Diffusion Monte Carlo Wave Functions to Analyze the Vibrational Spectra of $H_7O_3^+$ and $H_9O_4^+$. *J. Phys. Chem. A* **2021**, *125*, 7185–7197.

(31) Xantheas, S. S.; Dunning, T. H. Ab Initio Studies of Cyclic Water Clusters $(H_2O)_n$, $n = 1-6$. I. Optimal Structures and Vibrational Spectra. *J. Chem. Phys.* **1993**, *99*, 8774–8792.

(32) Miliordos, E.; Aprà, E.; Xantheas, S. S. Optimal Geometries and Harmonic Vibrational Frequencies of the Global Minima of Water Clusters $(H_2O)_n$, n= 2–6, and Several Hexamer Local Minima at the CCSD(T) Level of Theory. *J. Chem. Phys.* **2013**, *139*, 114302.

(33) Badger, R. M. A Relation Between Internuclear Distances and Bond Force Constants. *J. Chem. Phys.* **1934**, *2*, 128–131.

(34) Boyer, M. A.; Marsalek, O.; Heindel, J. P.; Markland, T. E.; McCoy, A. B.; Xantheas, S. S.

Beyond Badger's Rule: The Origins and Generality of the Structure–Spectra Relationship of Aqueous Hydrogen Bonds. *J. Phys. Chem. Lett.* **2019**, *10*, 918–924.

(35) Heindel, J. P.; Yu, Q.; Bowman, J. M.; Xantheas, S. S. Benchmark Electronic Structure Calculations for $H_3O^+(H_2O)_n$, $n = 0-5$, Clusters and Tests of an Existing 1,2,3-Body Potential Energy Surface with a New 4-Body Correction. *J. Chem. Theory Comput.* **2018**, *14*, 4553–4566.

(36) Gruenbaum, S. M.; Tainter, C. J.; Shi, L.; Ni, Y.; Skinner, J. L. Robustness of Frequency, Transition Dipole, and Coupling Maps for Water Vibrational Spectroscopy. *J. Chem. Theory Comput.* **2013**, *9*, 3109–3117.

(37) Ni, Y.; Skinner, J. L. IR and SFG Vibrational Spectroscopy of the Water Bend in the Bulk Liquid and at the Liquid-Vapor Interface, Respectively. *J. Chem. Phys.* **2015**, *143*, 014502.

(38) Kananenka, A. A.; Skinner, J. L. Fermi Resonance in OH-stretch Vibrational Spectroscopy of Liquid Water and the Water Hexamer. *J. Chem. Phys.* **2018**, *148*, 244107.

(39) Tainter, C. J.; Ni, Y.; Shi, L.; Skinner, J. L. Hydrogen Bonding and OH-Stretch Spectroscopy in Water: Hexamer (Cage), Liquid Surface, Liquid, and Ice. *J. Phys. Chem. Lett.* **2013**, *4*, 12–17.

(40) Hayashi, T.; la Cour Jansen, T.; Zhuang, W.; Mukamel, S. Collective Solvent Coordinates for the Infrared Spectrum of HOD in D_2O Based on an ab Initio Electrostatic Map. *J. Phys. Chem. A* **2005**, *109*, 64–82.

(41) Eaves, J. D.; Tokmakoff, A.; Geissler, P. L. Electric Field Fluctuations Drive Vibrational Dephasing in Water. *J. Phys. Chem. A* **2005**, *109*, 9424–9436.

(42) Yang, N.; Huchmala, R. M.; McCoy, A. B.; Johnson, M. A. Character of the OH Bend–Stretch Combination Band in the Vibrational Spectra of the "Magic" Number $H_3O^+(H_2O)_{20}$ and $D_3O^+(D_2O)_{20}$ Cluster Ions. *J. Phys. Chem. Lett.* **2022**, *13*, 8116–8121.

(43) Hermansson, K. Electric-field effects on the OH vibrational frequency and infrared absorption intensity for water. *J. Chem. Phys.* **1993**, *99*, 861–868.

(44) Diken, E. G.; Robertson, W. H.; Johnson, M. A. The Vibrational Spectrum of the Neutral $(H_2O)_6$ Precursor to the "Magic" $(H_2O)_6^-$ Cluster Anion by Argon-Mediated, Population-Modulated Electron Attachment Spectroscopy. *J. Phys. Chem. A* **2004**, *108*, 64–68.

(45) Finney, J. M.; DiRisio, R. J.; McCoy, A. B. Guided Diffusion Monte Carlo: A Method for Studying Molecules and Ions that Display Large Amplitude Vibrational Motions. *J. Phys. Chem. A* **2020**, *124*, 9567–9577.

(46) Eigen, M. Proton Transfer, Acid-Base Catalysis, and Enzymatic Hydrolysis. Part I: Elementary Processes. *Angew. Chem., Int. Ed. Engl.* **1964**, *3*, 1–19.

(47) Zundel, G. Hydrogen Bonds with Large Proton Polarizability and Proton Transfer Processes in Electrochemistry and Biology. *Adv. Chem. Phys.* **1999**, *111*, 1–217.

(48) Anderson, J. B. A Random-Walk Simulation of the Schrödinger Equation: H_3^+. *J. Chem. Phys.* **1975**, *63*, 1499–1503.

(49) Suhm, M. A.; Watts, R. O. Quantum Monte Carlo Studies of Vibrational States in Molecules and Clusters. *Phys. Rep* **1991**, *204*, 293 – 329.

(50) Barnett, R.; Reynolds, P.; W.A Lester, J. Monte Carlo Algorithms for Expectation Values of Coordinate Operators. *J. Comput. Phys.* **1991**, *96*, 258 – 276.

(51) Reynolds, P. J.; Ceperley, D. M.; Alder, B. J.; Lester, W. A. Fixed-Node Quantum Monte Carlo for Molecules. *J. Chem. Phys.* **1982**, *77*, 5593–5603.

(52) B. L. Hammond, J., W. A. Lester, Reynolds, P. J., Eds. *Monte Carlo Methods in Ab Initio Quantum Chemistry*; World Scientific Lecture and Course Notes in Chemistry; World Scientific Publishing Co.: Singapore, 1994; Vol. 1.

(53) DiRisio, R. J.; Finney, J. M.; McCoy, A. B. Diffusion Monte Carlo approaches for studying nuclear quantum effects in fluxional molecules. *WIREs Computational Molecular Science* **2022**, *12*, e1615.

(54) Lee, V. G. M.; McCoy, A. B. An Efficient Approach for Studies of Water Clusters Using Diffusion Monte Carlo. *J. Phys. Chem. A* **2019**, *123*, 8063–8070.

(55) Heine, N.; Fagiani, M. R.; Rossi, M.; Wende, T.; Berden, G.; Blum, V.; Asmis, K. R. Isomer-Selective Detection of Hydrogen-Bond Vibrations in the Protonated Water Hexamer. *J. Am. Chem. Soc.* **2013**, *135*, 8266–8273.

(56) Fournier, J. A.; Wolke, C. T.; Johnson, C. J.; Johnson, M. A.; Heine, N.; Gewinner, S.; Schöllkopf, W.; Esser, T. K.; Fagiani, M. R.; Knorke, H. et al. Site-Specific Vibrational Spectral Signatures of Water Molecules in the Magic $H_3O^+(H_2O)_{20}$ and $Cs^+(H_2O)_{20}$ Clusters. *Proceedings of the National Academy of Sciences* **2014**, *111*, 18132–18137.

(57) Buchanan, E. G.; Dean, J. C.; Zwier, T. S.; Sibert, E. L. Towards a first-principles model of Fermi resonance in the alkyl CH stretch region: Application to 1,2-diphenylethane and 2,2,2-paracyclophane. *J. Chem. Phys.* **2013**, *138*, 064308.

(58) Tabor, D. P.; Hewett, D. M.; Bocklitz, S.; Korn, J. A.; Tomaine, A. J.; Ghosh, A. K.; Zwier, T. S.; Sibert, E. L. Anharmonic Modeling of the Conformation-Specific IR Spectra of ethyl, n-propyl, and n-butylbenzene. *J. Chem. Phys.* **2016**, *144*, 224310.

(59) Frisch, M. J.; Trucks, G. W.; Schlegel, H. B.; Scuseria, G. E.; Robb, M. A.; Cheeseman, J. R.; Scalmani, G.; Barone, V.; Petersson, G. A.; Nakatsuji, H. et al. Gaussian 16 Revision C.01. 2016; Gaussian Inc. Wallingford CT.

(60) Fournier, J. A.; Wolke, C. T.; Johnson, M. A.; Odbadrakh, T. T.; Jordan, K. D.; Kathmann, S. M.; Xantheas, S. S. Snapshots of Proton Accommodation at a Microscopic Water Surface: Understanding the Vibrational Spectral Signatures of the Charge Defect in Cryogenically Cooled $H^+(H_2O)_{n=2-28}$ Clusters. *J. Phys. Chem. A* **2015**, *119*, 9425–9440.

(61) Boyer, M. A.; McCoy, A. B. A Wave Function Correction-Based Approach to the Identification of Resonances for Vibrational Perturbation Theory. submitted to *J. Chem. Phys.*, 2022.

(62) Duong, C. H.; Yang, N.; Kelleher, P. J.; Johnson, M. A.; DiRisio, R. J.; McCoy, A. B.; Yu, Q.; Bowman, J. M.; Henderson, B. V.; Jordan, K. D. Tag-Free and Isotopomer-Selective Vibrational Spectroscopy of the Cryogenically Cooled $H_9O_4^+$ Cation with Two-Color, IR–IR Double-Resonance Photoexcitation: Isolating the Spectral Signature of a Single OH Group in the Hydronium Ion Core. *J. Phys. Chem. A* **2018**, *122*, 9275–9284.

(63) Partridge, H.; Schwenke, D. W. The Determination of an Accurate Isotope Dependent Potential Energy Surface for Water from Extensive ab Initio Calculations and Experimental Data. *J. Chem. Phys.* **1997**, *106*, 4618–4639.

(64) Huang, X.; Carter, S.; Bowman, J. M. *Ab initio* Potential Energy Surface and Rovibrational Energies of H_3O^+ and its Isotopomers. *J. Chem. Phys.* **2003**, *118*, 5431–5441.

(65) Halonen, L.; Child, M. A Local Mode Model for Tetrahedral Molecules. *Mol. Phys.* **1982**, *46*, 239–255.

(66) Child, M. S.; Lawton, R. T. Local and Normal Vibrational States: a Harmonically Coupled Anharmonic-Oscillator Model. *Faraday Discuss. Chem. Soc.* **1981**, *71*, 273–285.

(67) Yu, Q.; Carpenter, W. B.; Lewis, N. H. C.; Tokmakoff, A.; Bowman, J. M. High-Level VSCF/VCI Calculations Decode the Vibrational Spectrum of the Aqueous Proton. *J. Phys. Chem. B* **2019**, *123*, 7214–7224.

(68) Yang, N.; Khuu, T.; Mitra, S.; Duong, C. H.; Johnson, M. A.; DiRisio, R. J.; McCoy, A. B.; Miliordos, E.; Xantheas, S. S. Isolating the Contributions of Specific Network Sites to the Diffuse Vibrational Spectrum of Interfacial Water with Isotopomer-Selective Spectroscopy of Cold Clusters. *J. Phys. Chem. A* **2020**, *124*, 10393–10406.

Table 1: Reference Values of the OH and OD Stretch Frequencies (in cm^{-1}) and Expectation Values of r_{OH} and r_{OD} (in Å) and Resulting Parameters, Used in the Spectral Mapping Method in Figures 3, 4, S4, and S5.

System	$\langle r_{OH}\rangle_{ref}$ [a,b]	ν_{ref}	$d\omega/dr_e$ [c]	dI/dr_e [d]	I_0 [e]
H_2O [f]	0.976	3706.50 [g]	−19.4	37.4	18.7
D_2O [f]	0.971	2727.19 [g]	−13.1	18.8	27.8
H_3O^+ [h]	0.992	3544.84 [i]	−19.9	19.4	1130
D_3O^+ [h]	0.987	2592.39 [i]	−14.2	10.5	573

[a] Calculated from the wave functions obtained from five independent guided DMC simulations with 5000 walkers, run for 20 000 time steps with a time step size of 1 a.u.
[b] Standard deviations for these values are < 0.001 Å.
[c] In units of cm^{-1}/(0.001 Å).
[d] In units of (km mol^{-1})/(0.001 Å).
[e] In units of km mol^{-1}.
[f] Based on the potential by Partridge and Schwenke.[63]
[g] Frequencies obtained from ref. 63.
[h] Based on the potential by Huang, Carter, and Bowman.[64]
[i] Frequencies obtained from ref. 64.

Table 2: Equilibrium Values of the OH and OD Frequencies (in cm^{-1}) and Bond Lengths (in Å) Used to Develop the Correlations in Figure 2.

System	r_e	ω_e(OH)	ω_e(OD)
H_2O	0.962	3883.00[a]	2822.28[a]
H_3O^+	0.980	3648.32[b]	2653.43[b]

[a] Average of the symmetric and antisymmetric stretch in an isolated water molecule.

[b] Average of the symmetric and antisymmetric stretches in an isolated hydronium molecule.

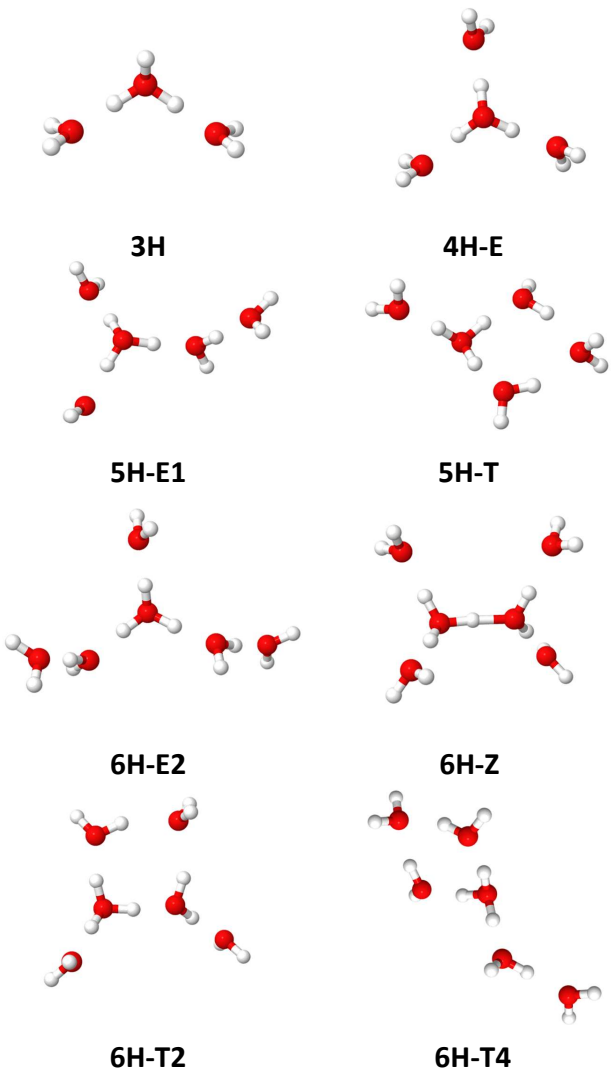

Figure 1: Equilibrium structures of the protonated water clusters that are the focus of this study. Structures were optimized using the potential energy surface developed by Yu and Bowman.[20] The corresponding coordinates can be found in Tables S23, S25, S28-S31 and S38-S43.

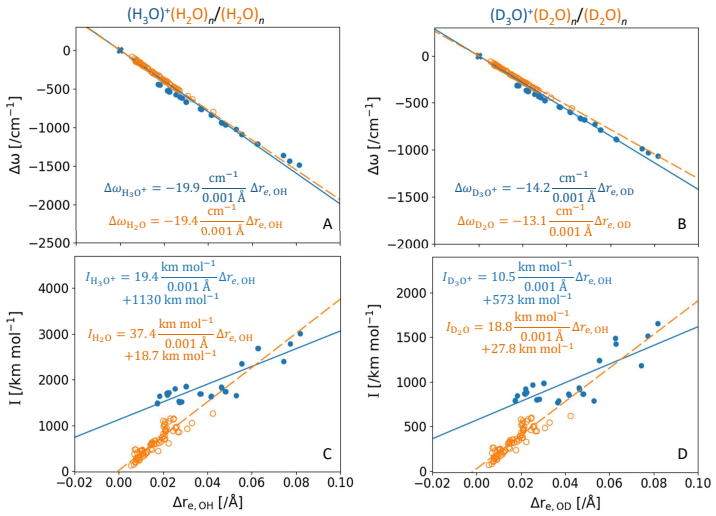

Figure 2: Plots showing the relationships between $\Delta\omega$ (A and B) and the harmonic intensity (C and D) and $\Delta r_{e,\mathrm{OH}}$ for the hydrogen bonded OH and OD stretches in isotopologues of $(H_2O)_n$, n=2-6, and $H^+(H_2O)_n$, n=3-6 shown in Figures S1 and S2. The values of $\Delta r_{e,\mathrm{OH}}$ and $\Delta\omega$ are obtained by subtracting the corresponding values for an OH bond in an isolated water molecule (orange) or hydronium ion (blue). The data is fit to the equations provided in the same color in the insets. The solid blue and open orange X in panels A and B represent the value of $\Delta\omega$ for the hydronium ion (blue) and the isolated water molecule (orange). The equilibrium values of $r_{e,\mathrm{OH}}$ and ω are provided in Table 2. The data used to make these plots are provided in the Excel file in the Supporting Information.

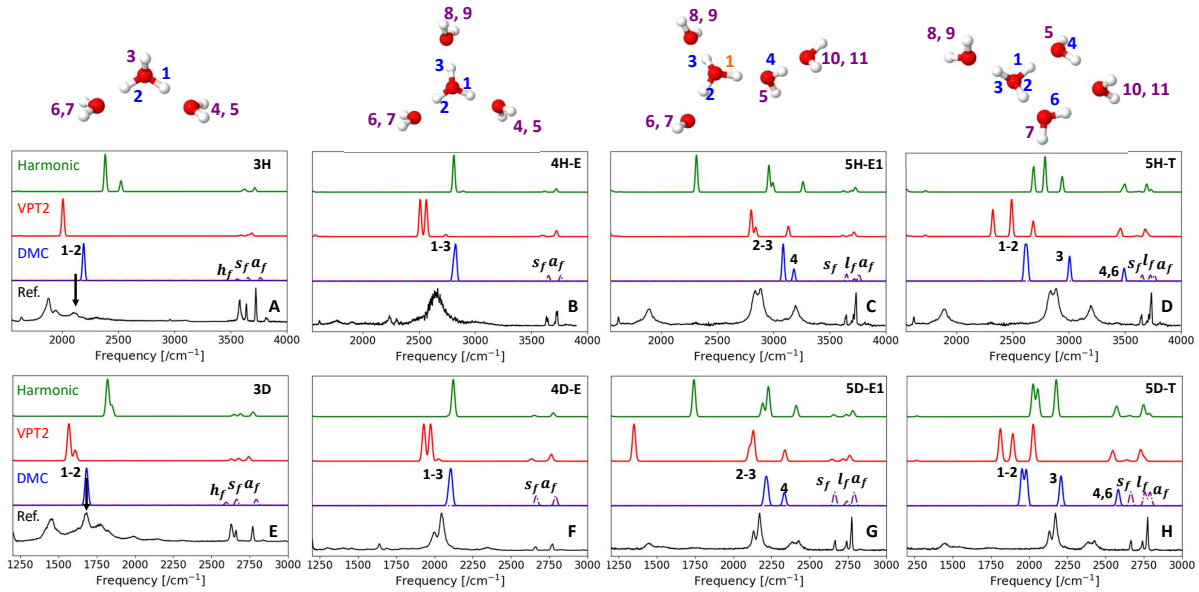

Figure 3: Comparisons of the calculated spectra of **3H** (A), **4H-E** (B), and two isomers of **5H**, **5H-E1** (C), and **5H-T** (D), shown above the corresponding panels. The corresponding spectra of the deuterated species are included in panels E-H. The spectra plotted in green and red reflect the results of scaled harmonic and VPT2 calculations performed at the MP2/aug-cc-pVTZ(-d) level of theory/basis set (see Tables S7-S14). The factors used to scale the harmonic calculations are 0.9531 and 0.9696 for OH and OD stretching vibrations, respectively. The spectra plotted in blue are calculated using the model described in the text based on the results reported in Tables 1 and S3-S6. The peaks in these spectra that are associated with excitation of hydrogen-bonded OH bonds are labeled by the number associated with the OH bond in the structures above the plots. The spectrum in the free OH region is shown with a purple dotted line and the peaks are labeled as hydronium, h_f, symmetric OH stretch in water, s_f, and antisymmetric stretch in water, a_f. The **H5** structures also have water molecules that form a single hydrogen bond and have one free OH oscillator, l_f. The black curves provide the experimentally measured spectra for **H3**,[4] **H4**,[62] and **H5**,[9] with the arrow in panels A and E showing the expected location of the OH stretch of the hydronium core in **H3** and **D3**, respectively, based on the analysis of the spectrum.[4]

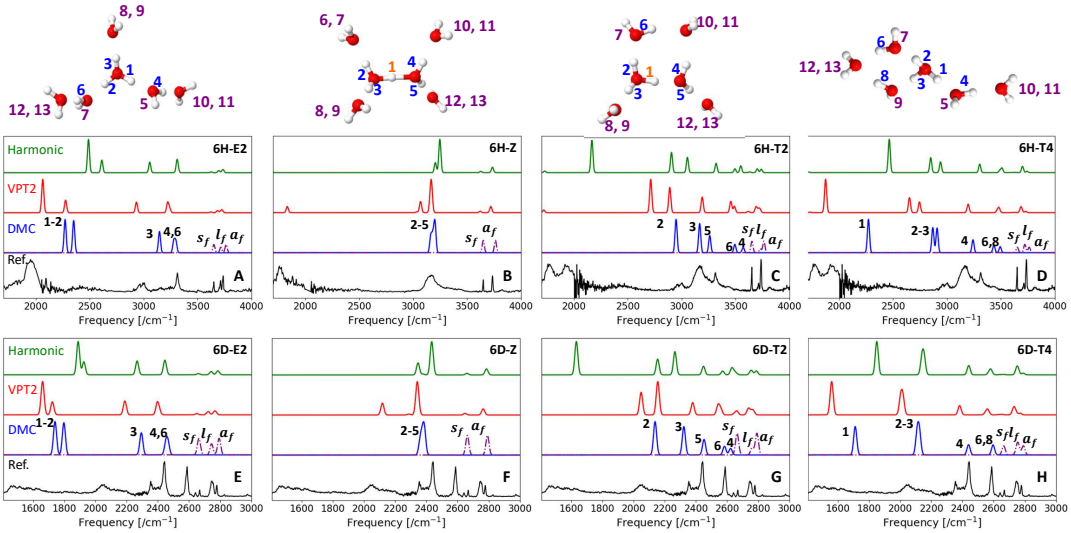

Figure 4: Same as Figure 3, but for **6H-E2** (A), **6H-T2** (B), **6H-Z** (C), and **6H-T4** (D). The spectra of the corresponding deuterated species are included in panels E-H. For comparison, in A and B, we show the spectra for **6H-E** and **6H-Z** obtained from double resonance experiments as black traces,[55] while the experimental spectra shown in the other panels are the raw spectra, which likely contain contributsion from multiple isomers.[2,55] The data used to generate the spectra shown in blue are provided in Tables S3-S6. The frequencies and intensities from the harmonic and VPT2 calculations are provided in Tables S15-S22, and the factors used to scale the harmonic calculations are 0.9531 and 0.9696 for OH and OD stretching vibrations, respectively. As in our previous study,[6] the peaks in the VPT2 spectrum for **6H-Z** at 3159 cm^{-1} and 3068 cm^{-1} as well as the peak in the VPT2 spectrum for **6D-Z** at 2339 cm^{-1} are shifted from their calculated VPT2 frequencies.

TOC graphic:

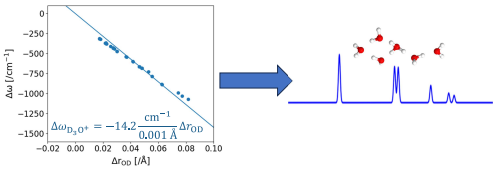
0
−250
−500
−750
−1000
−1250
−1500
Δω [/cm⁻¹]
−0.02 0.00 0.02 0.04 0.06 0.08 0.10
Δr_OD [/Å]
Δω_D3O+ = −14.2 cm⁻¹/0.001 Å Δr_OD